

Supporting Information

Multi-ring Aromatic Carbonyl Compounds Enabling High Capacity and Stable Performance of Sodium-Organic Batteries

Heng-guo Wang,^{a,b} Shuang Yuan,^{b,c} Zhenjun Si,^a and Xin-bo Zhang^{*b}

^aSchool of Materials Science and Engineering, Changchun University of Science and Technology, Changchun 130022, China

^bState Key Laboratory of Rare Earth Resource Utilization, Changchun Institute of Applied Chemistry, Chinese Academy of Sciences, Changchun 130022, China.

^cKey Laboratory of Automobile Materials, Ministry of Education, Department of Materials Science and Engineering, Jilin University, Changchun 130022, China.

Experimental Section

Materials: 3, 4, 9, 10-perylenetetracarboxylic dianhydride (PTCDA, 97%, Aldrich), 1,4,5,8-naphthalenetetracarboxylic dianhydride (NTCDA, 97%, Aldrich), pyromellitic dianhydride (PMDA, 97%, Aldrich), perylene (98%, Aldrich), pyrene (97%, Aldrich), truxene (98%, Aldrich), sodium hydroxide (NaOH, 98%, Aladdin Reagent), N-methylpyrrolidone (NMP, Aladdin Reagent, AR), acetylene black (Hong-xin Chemical Works), separator (polypropylene film, Celgard 2400), NaPF₆ (98%, Aldrich), ethylene carbonate (EC, 99%, Aldrich), dimethyl carbonate (DMC, ≥ 99%, Aldrich). All the reagents used in the experiment were of analytical grade purity and were used as received. De-ionized water with the specific resistance of 18.2 MΩ·cm was obtained by reversed osmosis followed by ion-exchange and filtration.

Synthesis of NaPTCDA: Tetrasodium salt of 3, 4, 9, 10-perylenetetracarboxylic dianhydride (NaPTCDA) was prepared from the reaction of 3, 4, 9, 10-perylenetetracarboxylic dianhydride (PTCDA) with NaOH, as illustrated in Fig. 1a. In a typical synthesis, PTCDA (3.92 g, 10 mmol) was added into deionized water (5 mL) containing NaOH (1.6 g, 40 mmol) at 50–60 °C. Deionized water (35 mL) was gradually added and the residue was dissolved. Then, EtOH was added to the solution until the precipitate was formed. After stirring the mixture for 12 h, the precipitate was collected by filtration, washed repeatedly by shaking with EtOH, and dried in vacuum at 100 °C for 12 h.

Theory Calculation: All the calculations were performed with the Gaussian 09 package.¹ The geometrical structures of the ground states were optimized at B3LYP/6-31 G(d) level² in gas phase by the Density functional theory (DFT).³

Characterization: FTIR measurements were performed on a Bruker IFS 66V/S spectrometer using KBr pellets. X-ray diffraction (XRD) patterns were recorded on a

Rigaku-Dmax 2500 diffractometer with Cu K α radiation. X-ray photoelectron spectroscopy (XPS) analysis was carried on an ESCALAB MK II X-ray instrument.

Electrochemical Measurements: The electrodes were prepared by mixing active material (60 wt%), acetylene black (30 wt%), and carboxyl methyl cellulose (CMC, 10 wt%) in deionized water. After the slurries were uniformly spread onto a copper foil, the electrodes were dried at 80 °C in vacuum for 8 h. The average mass loading of active materials was ca. 0.6 mg cm⁻². The electrodes were then pressed and cut into disks before transferring into an argon-filled glove box. Coin cells (CR2025) were assembled in the laboratory using sodium metal as the counter electrode, Celgard 2400 membrane as the separator, and NaPF₆ (1 M) in ethylene carbonate/dimethyl carbonate (EC/DMC, 1:1 w/w) as the electrolyte. Galvanostatic charge-discharge tests were carried out on a Land Battery Measurement System (Land, PR China). Cyclic voltammetry (CV) was performed by using a VMP3 Electrochemical Workstation (Bio-logic Inc.).

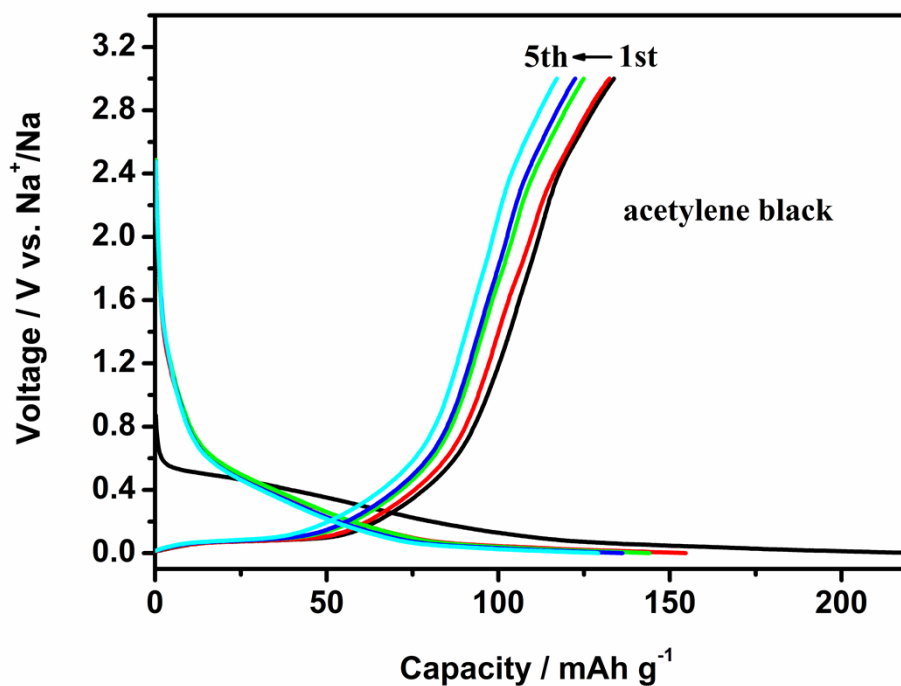


Fig. S1 Charge-discharge curves of acetylene black electrode at a current density of 25 mA g⁻¹ in the range 0-3 V. As shown in Fig. S1, the plateau at ca. 0.1 V is indicative of the reversible Na de/insertion into carbon and the acetylene black can deliver about 154 mAh g⁻¹. According to the literature,⁴ the capacity of 77 mAh g⁻¹ ($= 154 \text{ mAh g}^{-1} \times 30 \text{ wt\% of acetylene black} / 60 \text{ wt\% of PTCDA}$) is delivered from the conducting agent, acetylene black.

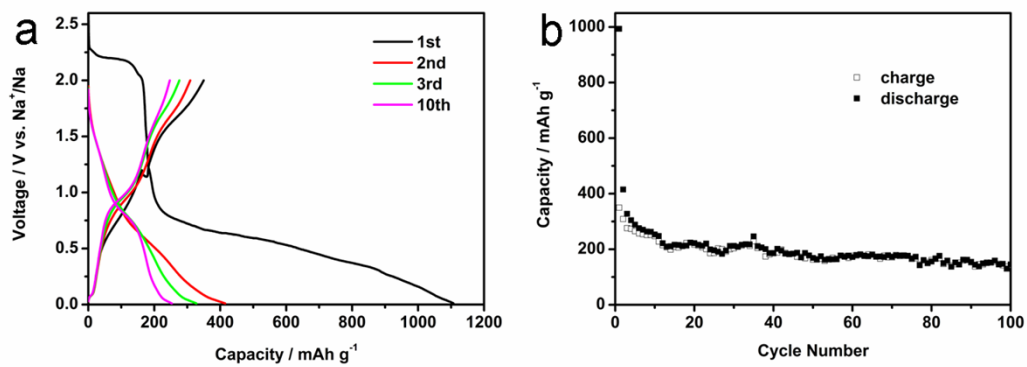


Fig. S2 (a) Charge-discharge curves and (b) cycle performance of PTCDA electrode at a current density of 25 mA g⁻¹ in the range 0-2 V.

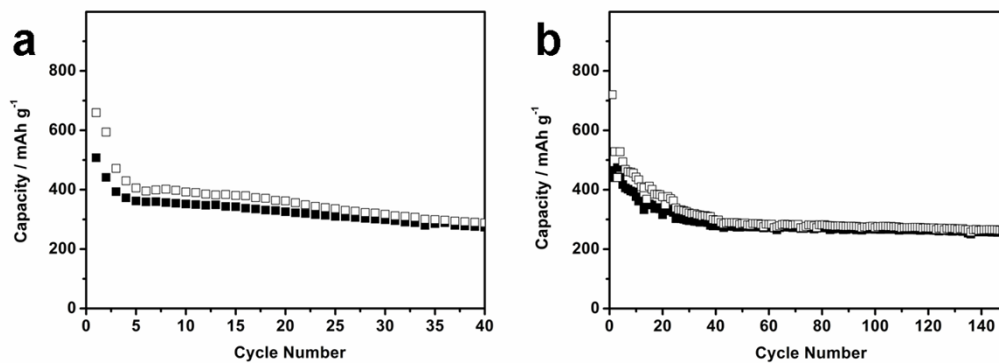


Fig. S3 Cycle performance of PTCDA at 55 °C at a current density of 25 mA g⁻¹ (a) and 100 mA g⁻¹ (b). Interestingly, at high temperature (55 °C), PTCDA can exhibit highly enhanced capacities of 719.9 and 659.3 mAh·g⁻¹ at the current densities of 25 and 100 mA·g⁻¹, respectively. This might be attributed to the decreasing battery resistance and increase of the ion mobility of the electrolyte at elevated temperature. However, at high temperature (55 °C), the cycling stability decreases, which could be attributed to the degradation of the electrode/electrolyte interface and the decomposition of the electrolyte promoted by high temperature. Such promising results clearly demonstrate that the PTCDA electrode is able to work properly in a wide temperature range.

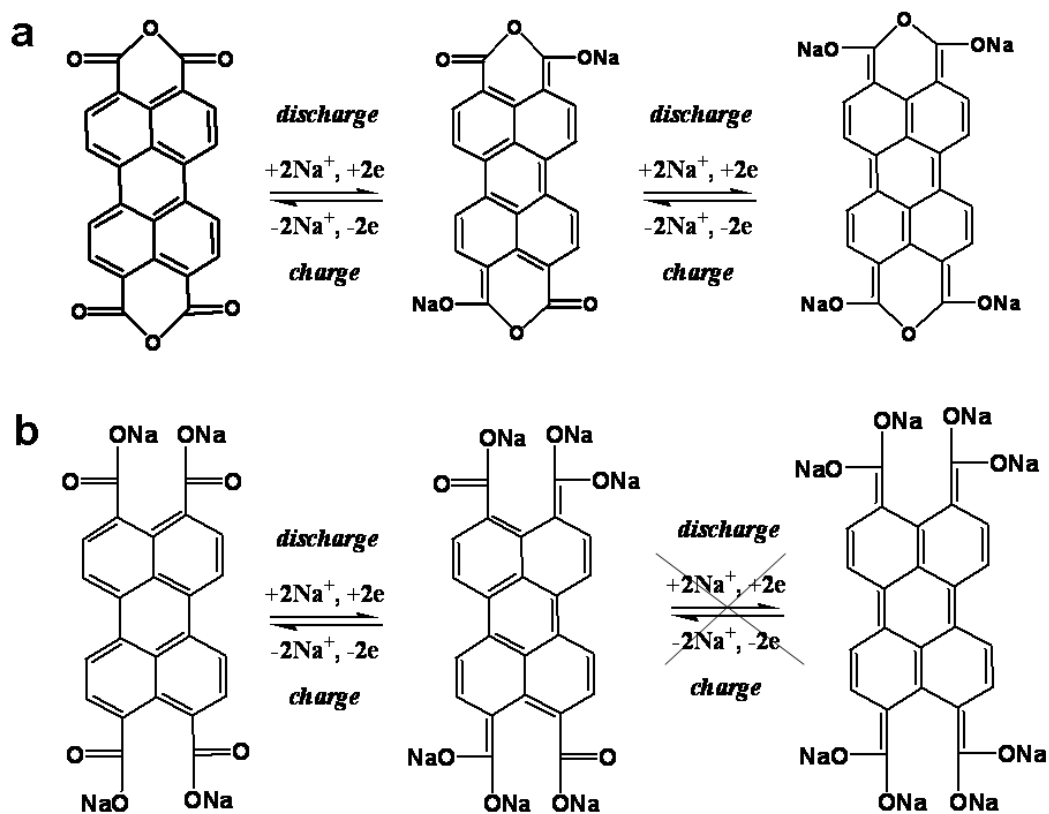


Fig. S4 Schematic diagram for the proposed reversible electrochemical redox mechanism of PTCDA (a) and NaPTCDA (b).

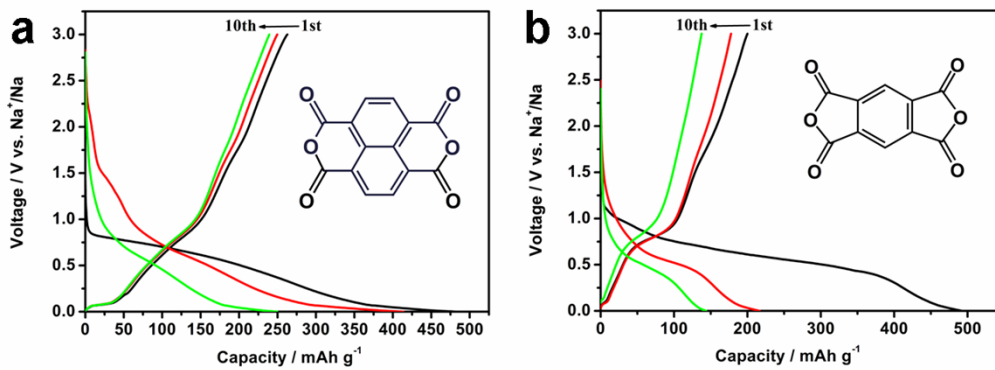


Fig. S5 Charge-discharge curves of NTCDA (a) and PMDA (b) at a current density of 25 mA g⁻¹ in the potential range of 0-3 V. It is obvious that the increase of benzene ring from PMDA to NTCDA and PTCDA has little impact on the capacity of these compounds. Therefore, this part of capacity might not be attributed to the addition reaction between Li/Na ions and the unsaturated carbon.

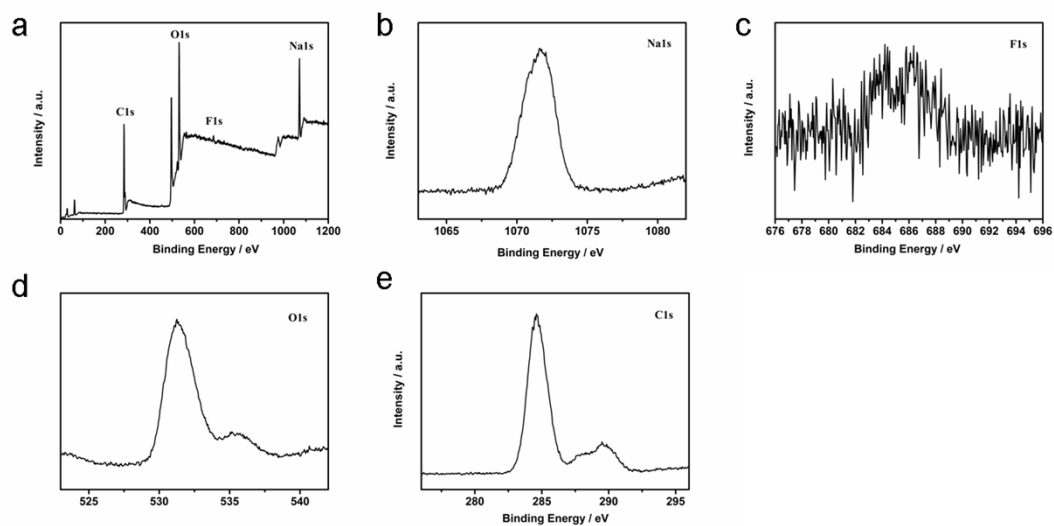


Fig. S6 Survey spectrum (a) and high-resolution Na1s (b), F1s (c), O1s(d), C1s (e) spectra of PTCDA electrode after 1st cycle discharge at 25 mA g⁻¹.

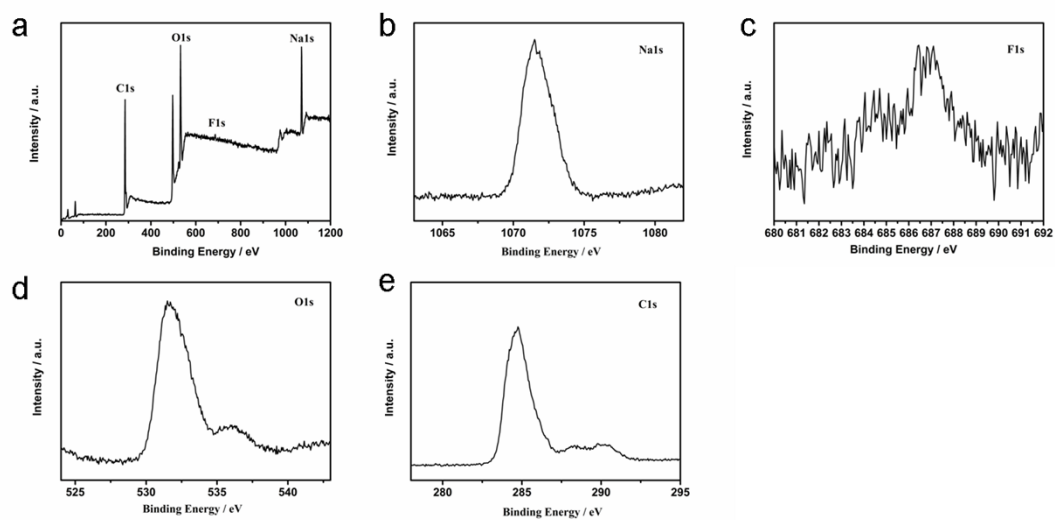


Fig. S7 Survey spectrum (a) and high-resolution Na1s (b), F1s (c), O1s(d), C1s (e) spectra of PTCDA electrode after 1st cycle charge at 25 mA g⁻¹.

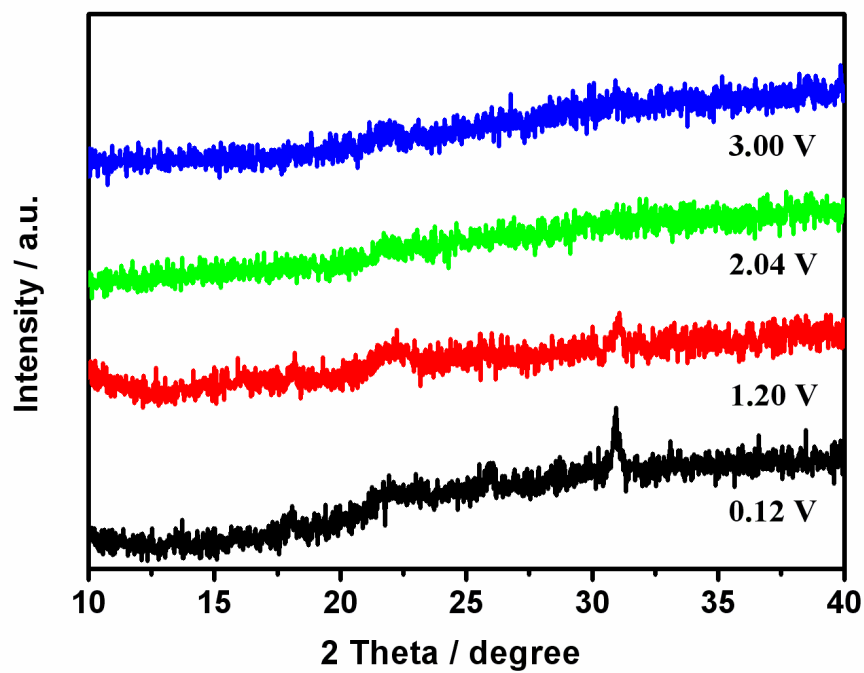


Fig. S8 Ex situ XRD patterns of PTCDA after first charge process.

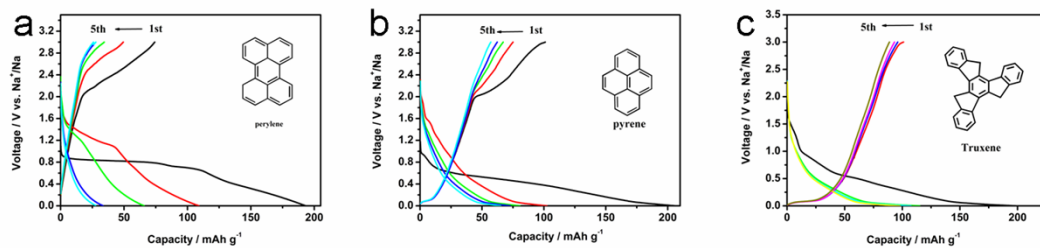


Fig. S9 Charge-discharge curves of perylene (a), pyrene (b), and truxene (c) at a current density of 25 mA g^{-1} .

References

- [1] M. J. Frisch, G. W. Trucks, H. B. Schlegel, G. E. Scuseria, M. A. Robb, J. R. Cheeseman, G. Scalmani, V. Barone, B. Mennucci, G. A. Petersson, H. Nakatsuji, M. Caricato, X. Li, H. P. Hratchian, A. F. Izmaylov, J. Bloino, G. Zheng, J. L. Sonnenberg, M. Hada, M. Ehara, K. Toyota, R. Fukuda, J. Hasegawa, M. Ishida, T. Nakajima, Y. Honda, O. Kitao, H. Nakai, T. Vreven, J. A. Jr Montgomery, J. E. Peralta, F. Ogliaro, M. Bearpark, J. J. Heyd, E. Brothers, K. N. Kudin, V. N. Staroverov, R. Kobayashi, J. Normand, K. Raghavachari, A. Rendell, J. C. Burant, S. S. Iyengar, J. Tomasi, M. Cossi, N. Rega, J. M. Millam, M. Klene, J. E. Knox, J. B. Cross, V. Bakken, C. Adamo, J. Jaramillo, R. Gomperts, R. E. Stratmann, O. Yazyev, A. J. Austin, R. Cammi, C. Pomelli, J. W. Ochterski, R. L. Martin, K. Morokuma, V. G. Zakrzewski, G. A. Voth, P. Salvador, J. J. Dannenberg, S. Dapprich, A. D. Daniels, O. Farkas, J. B. Foresman, J. V. Ortiz, J. Cioslowski, D. J. Fox, (2009) Gaussian 09 revision D.01. Gaussian Inc, Wallingford
- [2] A. Igor, M. Payam, C. Jérôme, C. D. Luisa, *J. Am. Chem. Soc.* **2007**, *129*, 8247.
- [3] E. Runge, E. K.U. Gross, *Phys. Rev. Lett.* **1984**, *52*, 997.
- [4] Y. Park, D. S. Shin, S. H. Woo, N. S. Choi, K. H. Shin, S. M. Oh, K. T. Lee, S. Y. Hong, *Adv. Mater.*, 2012, **24**, 3562.